Recent Results from IceCube and AMANDA

T. DeYoung
Department of Physics, Pennsylvania State University, University Park, PA 16802, USA
for the IceCube Collaboration

IceCube is a cubic kilometer neutrino telescope under construction at the South Pole, a successor to the first-generation AMANDA telescope. IceCube is now three quarters complete, with completion expected in early 2011, and data taken with the partially built detector already provides a sensitivity surpassing the complete AMANDA-II data set. Results from searches for astrophysical sources of neutrinos and for evidence of dark matter with both AMANDA and IceCube are summarized. We also discuss plans for Deep Core, an enhancement of IceCube designed to extend its sensitivity to neutrinos below the TeV scale.

1. Introduction

Nearly a century after the discovery of the cosmic rays, considerable uncertainty remains regarding the sources accelerating these particles. It is believed that cosmic rays at the highest energies, above the "ankle" in the cosmic ray spectrum around 10^{19} eV, are accelerated by extragalactic objects such as gamma ray bursts (GRBs) or active galactic nuclei (AGN). At lower energies, the sources of the cosmic rays are likely galactic objects such as supernova remnants (SNRs), although to date there is no conclusive evidence for cosmic ray acceleration by any of these objects.

The IceCube neutrino telescope, now under construction at the South Pole, attempts to detect very high energy (VHE, roughly TeV to PeV scale) neutrino emission from the accelerators of the cosmic rays. Neutrino emission is expected from such objects, since the highly energetic environments required to accelerate the cosmic rays will likely contain matter or radiation fields with which the accelerated hadrons may interact before escaping the source. These interactions will produce charged π and K mesons which decay to muon and electron neutrinos (and antineutrinos, which we will not distinguish in these proceedings) [1]. The neutrinos oscillate over distance between their sources and the Earth, leading to a general expectation of flavor equality at detection, although this is not guaranteed: deviations from flavor equality could provide a variety of information regarding the source environment or probe exotic fundamental physics.

At Earth, VHE neutrinos which undergo charged or neutral current interactions with a nucleon can be detected via the Cherenkov radiation emitted by secondary particles produced in the highly inelastic interaction. Neutrino flavor identification is possible based on the topology of the Cherenkov radiation: ν_μ charged current interactions produce a highly energetic muon that travels for hundreds of meters or kilometers on a straight trajectory, leading to long straight tracks in the detector. Electron neutrinos and neutral current interactions of all neutrinos produce localized showers of particles, leading to an approximately spherical emission of Cherenkov light. Tau neutrinos can produce a variety of signatures, depending on their energy and decay mode [2, 3, 4].

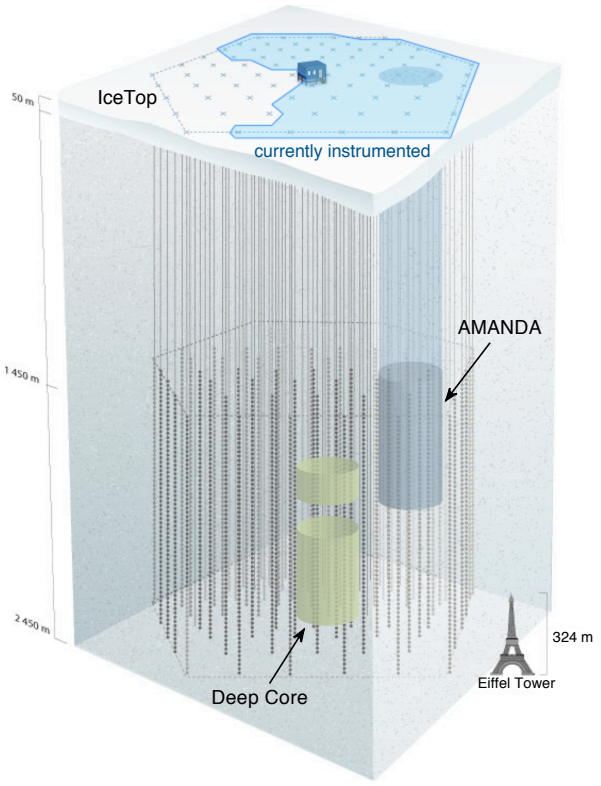

Figure 1: Schematic of the IceCube detector, including the initial AMANDA array, the new Deep Core low energy extension, and the IceTop air shower array. The portion of the detector installed as of 2009 is shown in blue, and the Eiffel Tower is shown for scale.

The IceCube telescope uses a cubic kilometer of the Antarctic ice cap as the Cherenkov medium to detect neutrinos, instrumenting the ice with a three dimensional array of photomultiplier tubes (PMTs) housed in digital optical modules (DOMs). The completed detector will consist of 5160 DOMs attached to 86 vertical strings at depths between 1450 m and 2450 m below the surface of the ice cap. In addi-

tion, an extensive air shower array on the surface, known as IceTop, will detect cosmic rays. The layout of the array is shown in Fig. 1. At present, 59 strings are installed and operational, with the remaining 27 strings to be deployed in the coming two austral summers. Also shown in Fig. 1 is the AMANDA telescope, which operated as an independent instrument from 2000-2006 and was integrated into IceCube from 2007-2008. AMANDA consisted of 687 optical modules on 19 strings, with the bulk of the detector at depths of 1500 to 2000 m. The AMANDA optical modules were simpler than their IceCube counterparts, with considerably smaller dynamic range and less ability to resolve individual photoelectrons. In 2009, AMANDA was decommissioned and the first string of its replacement, Deep Core, was deployed.

2. Atmospheric Neutrinos

The bulk of the neutrinos detected by IceCube are not produced in astrophysical accelerators, but rather in cosmic ray air showers in the Earth's atmosphere. These atmospheric neutrinos constitute a diffuse background to the astrophysical neutrinos from the cosmic ray sources, but they also provide a useful calibration beam for the detector. It is also possible to use the high-statistics atmospheric neutrino data set to make a variety of fundamental physics measurements [5]. Figure 2 shows the measurement of the atmospheric ν_μ spectrum extracted from the AMANDA seven year data set, as compared to two theoretical calculations [7, 8]. The spread between the two calculations does not indicate the full theoretical uncertainty, as both models rely on physics inputs which are themselves uncertain. AMANDA observes a spectrum which is slightly harder and slightly more numerous than the models, although consistent with the central values of the calculations at the 90% C.L. in normalization and the 99% C.L. in spectral index.

3. Point Sources of Neutrinos

The primary goal of IceCube is to detect individual sources of astrophysical neutrinos produced by cosmic ray accelerators. Such a source would be identifiable as a localized excess on the sky, normally with a harder energy spectrum than the atmospheric neutrino background. We search for sources using an unbinned (likelihood) approach. The true significance of deviations from the null hypothesis is assessed by generating an ensemble of background maps, using the real data set with every event scrambled in right ascension. Figure 3 shows the signficances of each point in the Northern Hemisphere sky produced by AMANDA in seven years of operation [9]. This data set includes 6,595 neutrino candidate events collected

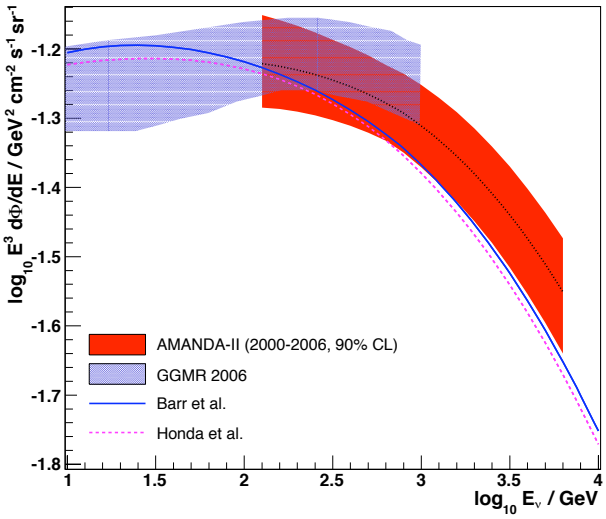

Figure 2: AMANDA measurement of the atmospheric $\nu_\mu + \bar{\nu}_\mu$ flux [5], compared to theoretical models (lines) and a measurement (GGMR) extracted from the Super-Kamiokande data [6]. The flux measured by AMANDA is slightly larger and harder than the Bartol calculation [7], but consistent at the 99% C.L. or better in each parameter. The total theoretical uncertainty is larger than the spread between the curves would suggest, due to uncertainties in measured parameters common to both calculations.

over 3.8 years of exposure (after accounting for readout dead time between events and summer maintenance periods). The most significant point in the map has a pre-trials significance equivalent to 3.38σ; a comparably significant point is found in 95% of scrambled background maps, indicating that the map is consistent with the absence of any neutrino point source.

A similar search was undertaken using the 2007 IceCube data set, containing 276 days of data from 22 strings taken between May 2007 and April 2008 [10]. A total of 5,114 neutrino candidate events was observed, consistent with an expectation of 4600 ± 1400 atmospheric neutrino events and 400 ± 200 cosmic ray muons misreconstructed as upgoing neutrino events. The same likelihood method was used to analyze the data, with the exception that the angular uncertainty was estimated for each neutrino event based on the width of the optimum in the likelihood space used to reconstruct the direction of the event, rather than using a generical overall angular resolution for all events. The resulting map of significances is shown in Figure 5. The most significant point in this map has a pre-trials significance of 7×10^{-7}; using randomized sky maps and also accounting for the fact that an independent search for emission from a list of candidate sources was also conducted using this data set, the probability of observing such a deviation from the null hypothesis is estimated at 1.34%, consistent with a background fluctuation.

The sensitivity of these searches is shown in Fig-

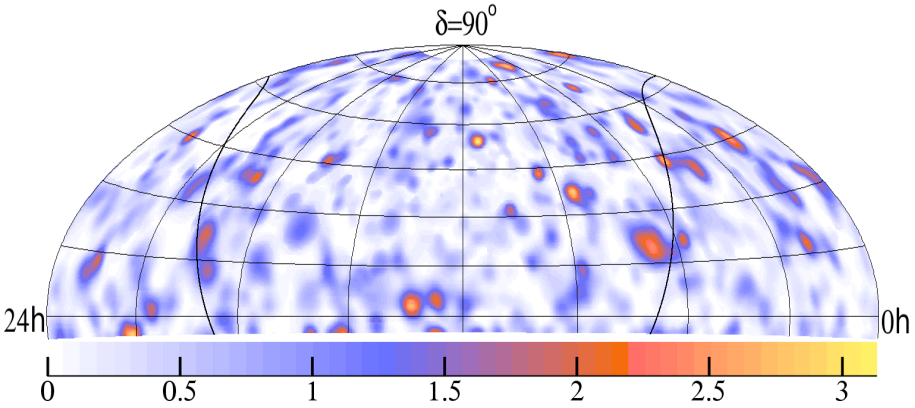

Figure 3: Map of the significances of deviations from the background in the AMANDA 2000-06 point source search. The scale converts these significances to standard deviations σ in the normal distribution. The most significant deviation is equivalent to 3.38σ before accounting for the number of points on the sky; a deviation at least this significant is found in 95% of scrambled (signal-free) sky maps, indicating that this observation is consistent with the background. The thin line indicates the Galactic plane.

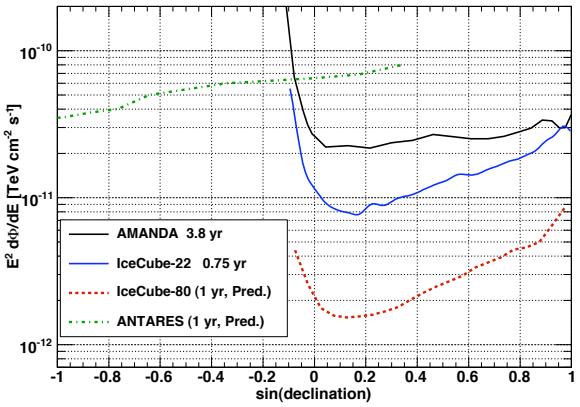

Figure 4: Average 90% C.L. upper limit on the $\nu_\mu + \bar{\nu}_\mu$ flux (assuming flavor equality) from a point source as a function of declination, compared to predicted sensitivities for IceCube and ANTARES.

ure 4, as a function of declination. The sensitivity of the IC22 search is significantly better than that of the AMANDA search, despite being based on a much shorter exposure (approximately 9 months of data collected in one year of operation, compared to 3.8 years of data collected in 7 years with AMANDA). The instantaneous sensitivity of IceCube, even when only one quarter built, is significantly better than that of AMANDA. The complete detector will be even more sensitive, a factor of five better than the present analysis with one year of operation.

A list of 26 potential neutrino emitters, known through their electromagnetic emissions, was drawn up *a priori*, including AGN, SNRs, and TeV gamma ray sources identified by Milagro in the Cygnus region [11] (now identified with GeV pulsars or pulsar wind nebulae [12] on the basis of correlations with the Fermi Bright Source List [13]). The likelihood ratio, as defined above, was calculated for each of these sources using the AMANDA data set. Because there are many fewer locations of interest, this restricted source is less subject to statistical trials penalties than the full-sky search, and is thus somewhat more sensitive. A similar analysis was performed on the IC22 data, using an expanded candidate list of 28 sources. A selection of the results from these searches is shown in Table I, including those with the smallest p-values in each search. In neither case are these p-values inconsistent with the background hypothesis: one expects to obtain $p \leq 0.0086$ for at least one of 26 sources in 20% of signal-free sky maps, and $p \leq 0.071$ in 66%. The 90% C. L. upper limits placed on ν_μ emission from the sources, assuming E^{-2} spectra and $1:1:1$ flavor ratios, are also shown in Table I.

4. Neutrinos from Gamma Ray Bursts

Searches for neutrino emission from gamma ray bursts were also conducted, using both the AMANDA and IceCube data sets. Because external detectors such as X-ray satellites detect the GRB, the IceCube search can be tailored carefully to the specific times and locations on the sky, leading to a drastically lower background rate. The expected event rates are also low, typically considerably less than one event per burst, so the searches are normally conducted by 'stacking' a collection of bursts and searching for neutrino emission from the ensemble as a whole.

The result of searches for emission from 419 GRBs observed in the Northern Hemisphere during stable AMANDA operations between 1997 and 2003 [14] is shown in Fig. 6. Three theoretical models are shown: the Waxman-Bahcall [15] (divided by 2 to account for neutrino oscillations) and Murase-Nagataki [16] cal-

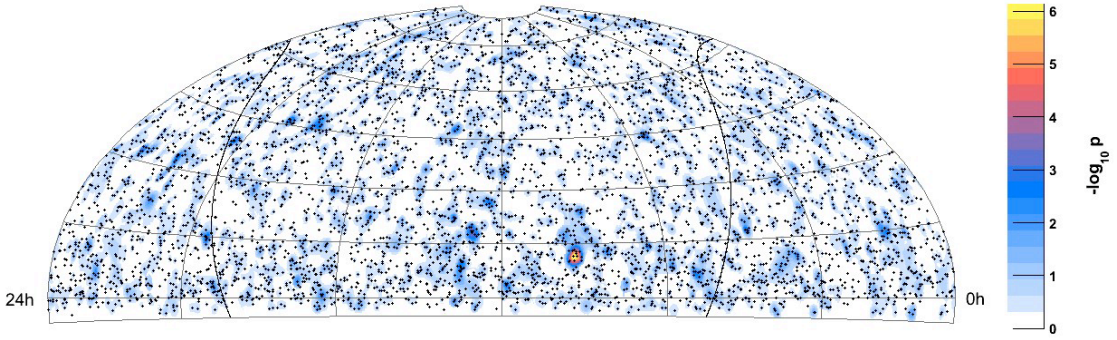

Figure 5: Map of significances on the northern sky in the 22-string 2007 IceCube point source search. Black dots indicate individual neutrino events, and the color scale indicates the significance of the likelihood ratio observed at each point. The most significant point on the sky has a significance (p-value) of 7×10^{-7}; there is a 1.34% chance of observing such a deviation under the background hypothesis, so this observation is consistent with background.

Table I Selected p-values and 90% C. L. upper limits on $\nu_\mu + \bar{\nu}_\mu$ fluxes $E_\nu^2\, dN/dE \leq \Phi_{90} \times 10^{-12}$ TeV/cm^2 s, from searches for neutrino emission from predefined candidate sources with AMANDA and IceCube-22. Dashes indicate that the p-value was not calculated because the best-fit number of signal events was zero.

Source	**decl. [°]**	**r.a. [h]**	**AMANDA p-value**	**IC22 p-value**	Φ_{90}**(AM)**	Φ_{90}**(IC22)**
Crab Nebula	22.01	5.58	0.10	–	46.4	10.35
Geminga	17.77	6.57	0.0086	–	63.9	9.67
MGRO J2019+37	36.83	20.32	0.077	0.25	48.4	25.23
LS I +61 303	61.23	2.68	0.034	–	73.7	22.00
XTE J1118+480	48.04	11.30	0.50	0.082	25.9	40.62
Cygnus X-1	35.20	19.97	0.57	–	20.0	14.60
Mrk 421	38.21	11.07	0.82	–	12.7	14.35
Mrk 501	39.76	16.90	0.22	–	36.4	14.44
1ES 1959+650	65.15	20.00	0.44	0.071	33.8	59.00
M87	12.39	12.51	0.43	–	22.5	7.91

culations based on the assumption that GRBs are the sources of the ultrahigh-energy cosmic rays, and a 'supranova' model [17] assuming that all GRBs are preceded by supernovae which produce ideal circumburst environments for neutrino production (only 60 GRB observations were used in placing this limit).

Because limits are placed on the integrated flux predicted by the models, our constraints are given in terms of "model rejection factors" (MRFs), essentially the scaling factor at which the model would be just ruled out at 90% confidence. MRFs less than 1 indicate that the model is excluded at the stated confidence level. The MRFs for the three models are 1.36 for the Waxman-Bahcall model, 0.92 for the Murase-Nagataki parameter set A, and 0.45 for the supranova model under the assumptions mentioned above.

The results of a comparable search using IceCube observations of 41 GRBs using the 22 string 2007 data set [18] are shown in Figure 7. Limits are placed on a model similar to the Waxman-Bahcall GRB prediction but taking into account the characteristics of individual bursts following the method of [19], as well as the precursor model of Razzaque et al. [20].

5. Diffuse Astrophysical Neutrino Fluxes

In addition to individual sources, one can also search for a diffuse flux of astrophysical neutrinos from an ensemble of sources too faint to resolve individually. Any such flux must be separated from the nearly isotropic flux of atmospheric neutrinos using the fact that the atmospheric spectrum is quite soft ($dN/dE \sim E^{-3.7}$) while the spectra of astrophysical sources are generically much harder (E^{-2} for ideal shock acceleration).

Two independent searches for diffuse fluxes were undertaken using AMANDA data. The first [21] was closely related to the standard muon neutrino analysis used to search for point sources of neutrinos, with cuts optimized for higher energy neutrinos and with a cut placed on the reconstructed energy of the neutrino

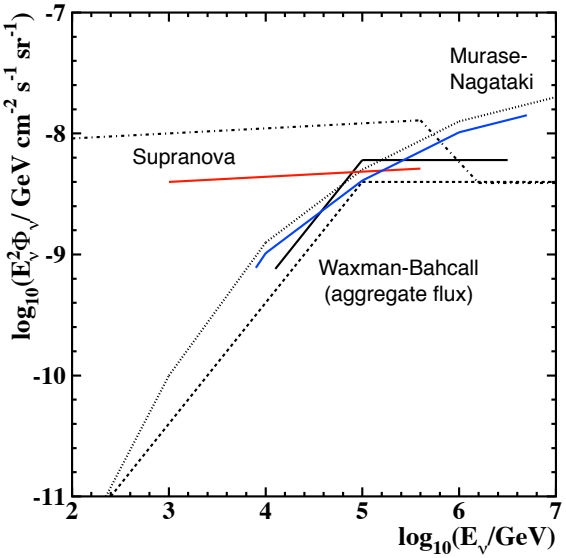

Figure 6: Integral limits at 90% C.L. on several $\nu_\mu + \bar{\nu}_\mu$ flux models (details in text) using AMANDA observations of 419 GRBs. Dashed lines indicate the model predictions, while solid lines show the relative level of the integral limit and the energy ranges of sensitivity. The energy ranges indicated contain 90% of the expected flux. The flux limits are for the full sky (4π sr), although only bursts from the Northern Hemisphere were used in the analysis.

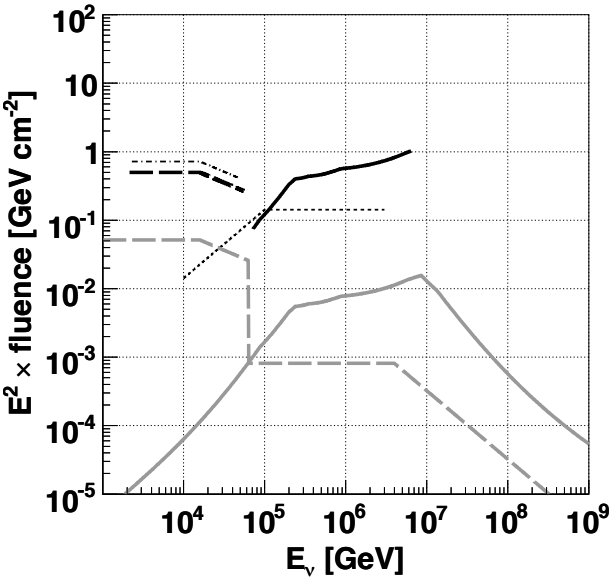

Figure 7: Integral limits (heavy black lines) at 90% C. L. on several predictions of total $\nu_\mu + \bar{\nu}_\mu$ fluence based on IceCube observations of 41 bursts with the 22 string 2007 configuration. The gray lines indicate the precursor model [20], peaked at lower energies, and our prediction for the prompt fluence (following [19]) at higher energies, using the observed characteristics of individual bursts in a Waxman-Bahcall like model. The solid lines show the relative level of the integral limits on these fluences, with the energy ranges indicated containing 90% of the expected fluence. The thin dotted lines are the AMANDA limits from Fig. 6 converted to fluences for comparison.

candidate events. This search used data from 2000–2003, and the results are shown in Fig. 8. As a benchmark, the limit placed on a hypothetical diffuse ν_μ flux $dN/dE = \Phi_0 E^{-2}$ at 90% C. L. is $\Phi_0 \geq 7.4 \times 10^{-8}$ GeV cm^{-2} s^{-1} sr^{-1}. For such a flux, 90% of the signal neutrinos would have had energies between 16 TeV and 2.5 PeV, which are the bounds of limit shown in Fig. 8. The limit is placed on the integrated flux, and so cannot be directly compared to specific theoretical models; instead, the predicted signal for each model must be simulated to find the model rejection factor (MRF). Limits on several specific models are also shown (as thin lines parallel to the predicted fluxes) in Fig. 8, and appear in Table II. In addition to astrophysical models, a flux corresponding to the upper bound on generic optically thin ($\tau_{n\gamma} < 1$) pion photoproduction sites [22] was tested. The upper limit from the analysis is a factor of 0.22 of the MPR bound over the region from 10 TeV to 630 TeV.

A second analysis based on data from 2000–2002 exploited idiosyncracies of the hardware response to the extremely bright events produced by ultrahigh energy (UHE) neutrinos, such as afterpulsing in the PMTs, to extend the range of the detector to much higher energies [31]. The limit for the E^{-2} benchmark ν_μ flux is 9.0×10^{-8} GeV cm^{-2} s^{-1} sr^{-1} at 90% C. L. (assuming a 1 : 1 : 1 flavor ratio), over a range from 2×10^5 GeV to 10^9 GeV, as shown in Fig. 8. It should be noted that the analysis was sensitive to all flavors of neutrinos; for a E^{-2} spectrum with flavor equality, the flavor ratio of the detected events would have been approximately 2 : 2 : 1. Limits on specific theoretical models are calculated separately for each model and are omitted from Fig. 8 for clarity but are shown in Table II.

Searches for diffuse astrophysical neutrinos are also underway using data from the 22-string 2007 configuration of IceCube (IC22) and the 40-string 2008 configuration (IC40). The IC22 sensitivity of 7.5×10^{-8} GeV cm^{-2} s^{-1} sr^{-1} is very nearly at the Waxman-Bahcall level, the benchmark diffuse flux level obtained by normalizing the parent proton population to the observed cosmic ray flux. The expected sensitivity from the IC40 data is well below the Waxman-Bahcall flux, indicating that the completed detector will probe astrophysically significant flux levels.

6. Search for Dark Matter

In addition to neutrinos produced during the acceleration of cosmic rays, IceCube would be sensitive to neutrinos produced in the decay of dark matter par-

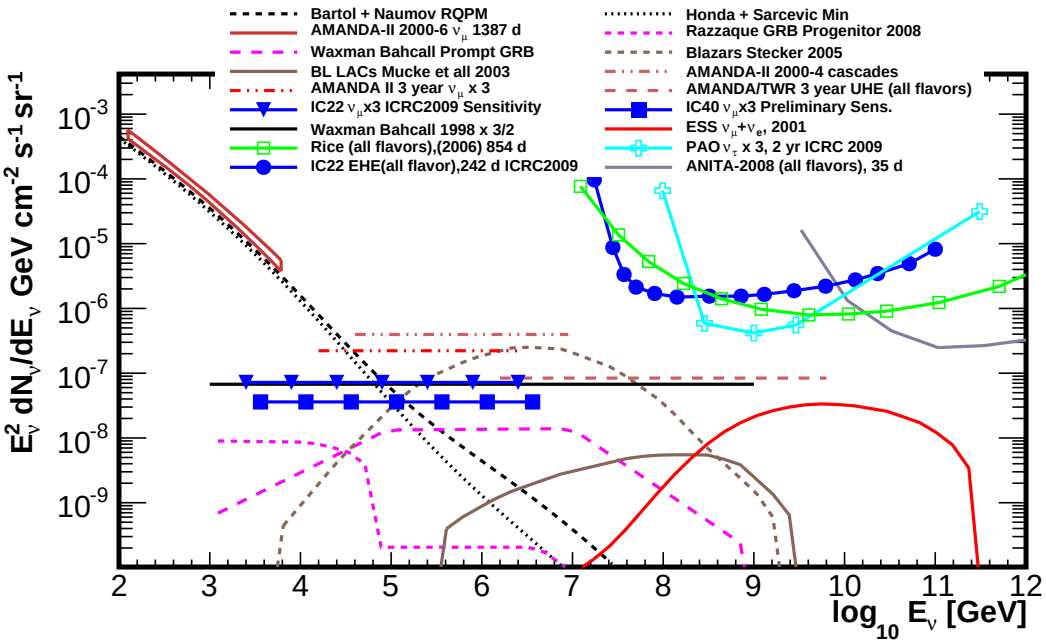

Figure 8: Limits on diffuse astrophysical neutrino fluxes from AMANDA and IceCube, compared with theoretical models and limits from other experiments. The AMANDA atmospheric muon neutrino measurement (Fig. 2) is the red region at upper left. Limits on possible E^{-2} diffuse fluxes from AMANDA, Baikal, and IceCube are shown as horizontal lines; these are integral limits on such fluxes, with the energy range from which the central 90% of the events would be expected shown. Fluxes which surpass those limits for only a small part of that energy range would not be excluded by these limits. Except for the atmospheric neutrinos, all fluxes include all flavors and have been rescaled if necessary assuming flavor equality at Earth. At upper right, a number of differential limits from ultrahigh energy neutrino experiments are shown; the levels of these limits are not directly comparable to the levels of the integral limits.

Table II Limits on several theoretical models of diffuse muon neutrino fluxes from the two AMANDA analyses. The number of events that would have been detected n_{sig} and the "model rejection factor" (MRF), the ratio of the upper limit to the predicted flux, are shown. MRFs less than 1 indicate that the model is excluded at the 90% C. L.

Source	n_{sig}**(HE)**	**MRF (HE)**	n_{sig}**(UHE)**	**MRF (UHE)**	**Model**
Active Galactic Nuclei	1.7	1.6	1.8	2.9	Stecker [23]
	1.4	2.0	5.9	0.9	MPR [22]
			8.8	0.6	Halzen & Zas [24]
			20.6	0.3	Protheroe [25]
			0.3	18.0	Mannheim [26] RL A
			4.5	1.2	Mannheim [26] RL B
Starburst Galaxies	1.1	21.1			Loeb & Waxman [27]
Prompt Atmospheric ν_μ	0.4	60.3			MRS GBW [28]
	4.7	5.2			Naumov RQPM [29]
	16.1	1.5			Zas et al. [30] Charm C
	26.2	0.95			Zas et al. [30] Charm D

ticles. For example, weakly interacting dark matter particles (WIMPs) such as neutralinos could scatter off nucleons in the Sun and become trapped in the solar gravitational well, where they could produce high energy neutrinos through various annihilation channels. Such a search is highly complementary to direct dark matter searches using heavy elements such as germanium or xenon, which seek to take advantage of coherent scattering of the WIMP off the nucleons in the atom. If the nucleon-WIMP scattering is independent of the nucleon spin (SI), then this coherence will increase the cross section σ_{SI} by a factor of the square of the atomic mass of the target. However, if the primary coupling is spin-dependent (SD), coherence is

lost and the cross section σ_{SD} will be much smaller. WIMP capture in the Sun, which is primarily made of light nuclei, provides a useful probe of models where the scattering is primarily spin-dependent [32].

It should be noted that, as opposed to direct dark matter detection experiments, in this indirect approach assumptions must be made regarding the annihilation products, which will affect the energy spectrum of the neutrinos emerging from such processes. The hardest spectrum would come from annihilations to W^+W^- ($\tau^+\tau^-$ for the lowest masses) and the softest from annihilations to $b\bar{b}$, so as limiting cases we assume the WIMPs decay exclusively to those particles. The actual annihilation cross section is irrelevant so long as the Sun is old enough for the WIMP population to have reached equilibrium, with captures balancing annihilations.

Searches for high energy neutrinos from the Sun have been undertaken with both AMANDA [33] and IC22 [34]. The limits on the SD scattering cross section produced by these searches are shown in Figure 9, in the limiting cases of hard and soft annihilation spectra. Limits from Super-Kamiokande [35] and a number of direct search experiments [36, 37, 38, 39] are also shown, as well as the allowed MSSM neutralino parameter space based on direct detection limits on the SI cross section. Tighter SI limits would rule out only a limited region of the allowed space, so IceCube provides a useful counterpart to future direct detection experiments.

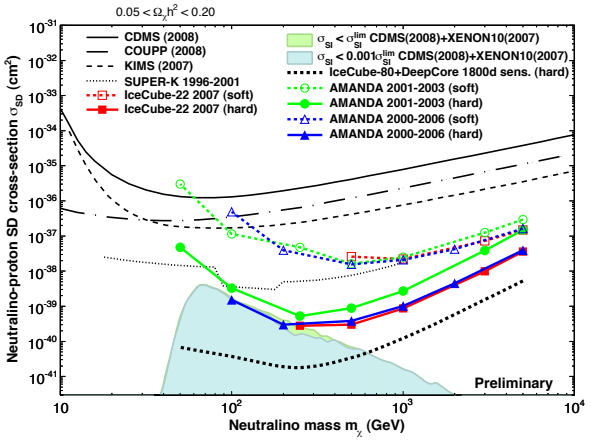

Figure 9: Limits on the spin-dependent neutralino-proton cross section derived by searching for high energy neutrinos from WIMP annihilation in the Sun. The limits are shown for the extreme cases of hard ($\chi\chi \to W^+W^-$) and soft ($b\bar{b}$) neutrino spectra. The shaded region indicates the MSSM parameter space allowed by existing limits on the corresponding spin-independent cross section predicted for that combination of SUSY parameters. The thin green shaded region would be ruled out if existing limits on σ_{SI} are improved by a factor of 10^3.

In the future, the low energy response of the IceCube detector will be greatly augmented by the addition of the Deep Core low energy extension, visible in Fig. 1. Deep Core will comprise the seven innermost standard IceCube strings, as well as six new strings deployed in a ring of radius 72 m around the central string. The six new strings will each mount 60 DOMs, 50 of which will be deployed on a 7 m spacing between 2100 m and 2450 m below the surface. The remaining 10 DOMs will be deployed at shallower depths to improve the efficiency of detection of extremely vertical background muons. With a radius of 125 m and a height of 350 m, the instrumented volume of Deep Core will instrument 15 Mton of ice, with expected sensitivity to neutrinos at energies as low as ∼10 GeV.

The new DOMs will be identical to standard IceCube DOMs except that they will use a new model of PMT developed by Hamamatsu to increase the quantum efficiency of the photocathode. Lab tests with assembled DOMs indicate the sensitivity of the high-QE PMTs is approximately 30% higher than that of standard DOMs. The denser DOM spacing and higher DOM sensitivity combined will increase the collection of photons in the Deep Core volume by approximately a factor of 5. Furthermore, the ice at Deep Core depths is significantly more transparent than that at shallower depths, with optical attenuation lengths of 40–45 m compared to 20–25 m in the top of the detector. The significantly improved light collection in Deep Core translates to much higher sensitivity to relatively dim, low energy neutrino events. Additionally, the bulk of IceCube can be used to detect and veto atmospheric muons penetrating to Deep Core. The ratio of the atmospheric muon trigger rate to the atmospheric neutrino trigger rate in IceCube is approximately 10^6; initial Monte Carlo studies indicate that veto efficiencies on this order are achievable with relatively good signal efficiency.

The first of the six new Deep Core strings was successfully deployed at South Pole in the 2008-09 austral summer. Preliminary evaluations of the performance of the hardware *in situ* confirm expectations from laboratory studies. Deployment of the remaining five new strings, as well as the standard strings that compose the Deep Core array, is scheduled to be complete by February 2010. Deep Core will enable study of a number of topics in neutrino physics and searches for neutrinos from point sources in the southern sky, including the Galactic center region. It will also greatly improve the sensitivity of IceCube to low-mass WIMPs. A preliminary sensitivity curve for Deep Core using 1800 days of data is shown in Fig. 9.

7. Outlook

IceCube construction is proceeding well, with completion expected in 2011. IceCube will be augmented with the Deep Core array, to be completed in 2010, which will extend its capabilities to energies as low

as 10 GeV. Initial results from the partially built detector, including only one quarter of the final array, are already providing sensitivities beyond those of the complete seven-year AMANDA-II data set, and this sensitivity will improve rapidly as construction progresses. Within a few years the sensitivity of IceCube will be sufficient to probe astrophysical neutrino fluxes below the Waxman-Bahcall level. In addition, IceCube and Deep Core will permit indirect searches for dark matter well beyond existing limits.

Acknowledgments

We acknowledge the support from the following agencies: U.S. National Science Foundation-Office of Polar Program, U.S. National Science Foundation-Physics Division, University of Wisconsin Alumni Research Foundation, U.S. Department of Energy, and National Energy Research Scientific Computing Center, the Louisiana Optical Network Initiative (LONI) grid computing resources; Swedish Research Council, Swedish Polar Research Secretariat, and Knut and Alice Wallenberg Foundation, Sweden; German Ministry for Education and Research (BMBF), Deutsche Forschungsgemeinschaft (DFG), Germany; Fund for Scientific Research (FNRS-FWO), Flanders Institute to encourage scientific and technological research in industry (IWT), Belgian Federal Science Policy Office (Belspo); the Netherlands Organisation for Scientific Research (NWO); M. Ribordy acknowledges the support of the SNF (Switzerland); A. Kappes and A. Groß acknowledge support by the EU Marie Curie OIF Program.

References

[1] J. G. Learned and K. Mannheim, *Ann. Rev. Nucl. Part. Sci.* **50**, 679 (2000).
[2] J. G. Learned and S. Pakvasa, *Astropart. Phys.* **3**, 267 (1995).
[3] J. F. Beacom, N. F. Bell, D. Hooper, S. Pakvasa and T. J. Weiler, *Phys. Rev. D* **68**, 093005 (2003) [Erratum-ibid. *D* **72**, 019901 (2005)].
[4] T. DeYoung, S. Razzaque and D. F. Cowen, *Astropart. Phys.* **27**, 238 (2007).
[5] R. Abbasi *et al.* [IceCube Collaboration], *Phys. Rev. D* **79**, 102005 (2009)
[6] M. C. Gonzalez-Garcia, M. Maltoni and J. Rojo, *JHEP* **0610**, 075 (2006).
[7] G. D. Barr *et al.*, *Phys. Rev. D* **70**, 023006 (2004).
[8] M. Honda *et al.*, *Phys. Rev. D* **75**, 043006 (2007).
[9] R. Abbasi *et al.* [IceCube Collaboration], *Phys. Rev. D* **79**, 062001 (2009).
[10] R. Abbasi *et al.* [IceCube Collaboration], *Astrophys. J.* **701**, L47 (2009)
[11] A. A. Abdo *et al.* [Milagro Collaboration], *Astrophys. J.* **664**, L91 (2007).
[12] A. A. Abdo *et al.*, *Astrophys. J.* **700**, L127 (2009) [Erratum-ibid. **703**, L185 (2009)]
[13] A. A. Abdo *et al.* [Fermi LAT Collaboration], *Astrophys. J. Suppl.* **183**, 46 (2009)
[14] A. Achterberg and K. Hurley [The IceCube Collaboration and the IPN Collaboration], *Astrophys. J.* **674**, 357 (2008)
[15] E. Waxman, *Nucl. Phys. Proc. Suppl.* **118**, 353 (2003).
[16] K. Murase and S. Nagataki, *Phys. Rev. D* **73**, 063002 (2006).
[17] S. Razzaque, P. Meszaros and E. Waxman, *Phys. Rev. Lett.* **90**, 241103 (2003).
[18] R. Abbasi *et al.* [IceCube Collaboration], arXiv:0907.2227 [astro-ph.HE].
[19] D. Guetta, D. Hooper, J. Alvarez-Muniz, F. Halzen and E. Reuveni, *Astropart. Phys.* **20**, 429 (2004)
[20] S. Razzaque, P. Meszaros and E. Waxman, *Phys. Rev. D* **68**, 083001 (2003)
[21] A. Achterberg *et al.* [IceCube Collaboration], *Phys. Rev. D* **76**, 042008 (2007) [Erratum-ibid. D **77**, 089904 (2008)].
[22] K. Mannheim, R. J. Protheroe and J. P. Rachen, *Phys. Rev. D* **63**, 023003 (2001).
[23] F. W. Stecker, *Phys. Rev. D* **72**, 107301 (2005).
[24] F. Halzen and E. Zas, *Astrophys. J.* **488**, 669 (1997).
[25] R. J. Protheroe, arXiv:astro-ph/9607165.
[26] K. Mannheim, *Astropart. Phys.* **3**, 295 (1995).
[27] A. Loeb and E. Waxman, *JCAP* **0605**, 003 (2006).
[28] A. D. Martin, M. G. Ryskin and A. M. Stasto, *Acta Phys. Polon. B* **34**, 3273 (2003).
[29] V. A. Naumov, arXiv:hep-ph/0201310.
[30] E. Zas, F. Halzen and R. A. Vazquez, *Astropart. Phys.* **1**, 297 (1993).
[31] M. Ackermann *et al.* [IceCube Collaboration], *Astrophys. J.* **675**, 1014 (2008).
[32] F. Halzen and D. Hooper, *Phys. Rev. D* **73**, 123507 (2006).
[33] M. Ackermann *et al.* [AMANDA Collaboration], *Astropart. Phys.* **24**, 459 (2006).
[34] R. Abbasi *et al.* [IceCube Collaboration], *Phys. Rev. Lett.* **102**, 201302 (2009)
[35] S. Desai *et al.* [Super-Kamiokande Collaboration], *Phys. Rev. D* **70**, 083523 (2004) [Erratum-ibid. D **70**, 109901 (2004)].
[36] Z. Ahmed *et al.* [CDMS Collaboration], *Phys. Rev. Lett.* **102**, 011301 (2009).
[37] J. Angle *et al.* [XENON Collaboration], *Phys. Rev. Lett.* **100**, 021303 (2008).
[38] H. S. Lee. *et al.* [KIMS Collaboration], *Phys. Rev. Lett.* **99**, 091301 (2007).
[39] E. Behnke *et al.* [COUPP Collaboration], *Science* **319**, 933 (2008).